HOKKAIDO UNIVERSITY

Title	Quantification of Hand Synovitis in Rheumatoid Arthritis: Arterial Mask Subtraction Reinforced With Mutual Information Can Improve Accuracy of Pixel-by-Pixel Time-Intensity Curve Shape Analysis in Dynamic MRI
Author(s)	Kobayashi, Yuto; Kamishima, Tamotsu; Sugimori, Hiroyuki et al.
Citation	Journal of magnetic resonance imaging, 48(3), 687-694 https://doi.org/10.1002/jmri.25995
Issue Date	2018-09
Doc URL	https://hdl.handle.net/2115/75600
Rights	This is the peer reviewed version of the following article: Kobayashi, Y., Kamishima, T., Sugimori, H., Ichikawa, S., Noguchi, A., Kono, M., Iiyama, T., Sutherland, K. and Atsumi, T. (2018), Quantification of hand synovitis in rheumatoid arthritis: Arterial mask subtraction reinforced with mutual information can improve accuracy of pixel-by-pixel time-intensity curve shape analysis in dynamic MRI. J. Magn. Reson. Imaging, 48(3): 687-694, which has been published in final form at https://doi.org/10.1002/jmri.25995. This article may be used for non-commercial purposes in accordance with Wiley Terms and Conditions for Self-Archiving.
Type	journal article
File Information	JMRI_48(3)_687-694.pdf

Hokkaido University Collection of Scholarly and Academic Papers : HUSCAP

Title; Quantification of hand synovitis in rheumatoid arthritis: arterial mask subtraction reinforced with mutual information can improve accuracy of pixel by pixel time-intensity curve shape analysis in dynamic MRI

Author Names and Degrees; Yuto Kobayashi, RT[1], Tamotsu Kamishima, MD, PhD[2], Hiroyuki Sugimori, RT, PhD[2], Shota Ichikawa, RT, MS[3], Atsushi Noguchi, MD, PhD[3], Michihito Kono, MD, PhD[3], Toshitake Iiyama[5], RT, Kenneth Sutherland, PhD[6], Tatsuya Atsumi, MD, PhD[4]

Author Affiliations;

1, Graduate School of Health Sciences, Hokkaido University, Sapporo, Japan

2, Faculty of Health Sciences, Hokkaido University, Sapporo, Japan

3, Department of Radiological Technology, Kurashiki Central Hospital

4, Department of Rheumatology, Endocrinology and Nephrology, Graduate School of Medicine and Faculty of Medicine, Hokkaido University, Japan

5, Yaesu Clinic, Tokyo, JAPAN.

6, Global Station for Medical Science and Engineering, Global Institution for Collaborative Research and Education (GI-CoRE), Hokkaido University, Japan

Corresponding Author; Tamotsu Kamishima, Faculty of Health Sciences, Hokkaido University, Kita 12 Nishi 5, Kita-ku, Sapporo City 060-0812, Japan, TEL/FAX; +81-11-706-2824, E-mail; ktamotamo2@yahoo.co.jp.

Acknowledgments; We appreciate Taro Sakashita, RT, MS, Application Group, CT Sales Department, National Sales Division, Toshiba Medical Systems Corporation, Japan for his technical support.

Grant Support; NA

Running Title; Quantification of hand synovitis

Title; Quantification of hand synovitis in rheumatoid arthritis: arterial mask subtraction reinforced with mutual information can improve accuracy of pixel by pixel time-intensity curve shape analysis in dynamic MRI

Abstract

BACKGROUND: Synovitis, which is a hallmark of rheumatoid arthritis (RA), needs to be precisely quantified to determine the treatment plan. Time intensity curve (TIC) shape analysis is an objective assessment method for characterizing the pixels as artery, inflamed synovium, or other tissues using dynamic contrast enhanced MRI (DCE-MRI).

PURPOSE/HYPOTHESIS: To assess the feasibility of our original arterial mask subtraction method (AMSM) with mutual information (MI) for quantification of synovitis in RA.

STUDY TYPE: Prospective study.

SUBJECTS: Ten RA patients (9 women and 1 man; mean age, 56.8 years; range, 38-67 years).

FIELD STRENGTH/SEQUENCE: 3T/DCE-MRI

ASSESSMENT: After optimization of TIC shape analysis to the hand region, a combination of TIC shape analysis and AMSM was applied to synovial quantification. The MI between pre- and post-contrast images was utilized to determine the arterial mask phase objectively, which was compared with human subjective selection. Volume of objectively measured synovitis by software was compared with that of manual outlining by an experienced radiologist. Simple TIC shape analysis and TIC shape

analysis combined with AMSM were compared in slices without synovitis according to subjective evaluation.

STATISTICAL TESTS: Pearson's correlation coefficient, paired t-test and intra-class correlation coefficient (ICC).

RESULTS: TIC shape analysis was successfully optimized in the hand region with a correlation coefficient of 0.725 ($p<0.01$) with the results of manual assessment were regarded as ground truth. Objective selection utilizing MI had substantial agreement (ICC =0.600) with subjective selection. Correlation of synovial volumetry in combination with TIC shape analysis and AMSM with manual assessment was excellent ($r= .922$, $p<0.01$). In addition, negative predictive ability in slices without synovitis pixels was significantly increased ($p<0.01$).

DATA CONCLUSION: The combination of TIC shape analysis and image subtraction reinforced with MI can accurately quantify synovitis of RA in the hand by eliminating arterial pixels.

Keywords

Dynamic contrast-enhanced MRI, Time-intensity curve shape analysis, Rheumatoid arthritis, Mutual information, Synovitis quantification

Introduction

Rheumatoid arthritis (RA) is an autoimmune disease with chronic inflammation of synovial joints. In most cases of RA, synovitis behaves as a trigger to joint destruction (1). As a result of the progression of synovitis, joint pain, stiffness, accompany permanent damage which may cause patients a decrease in their quality of life (1). Detection of synovitis and evaluation of its status therefore play important roles in deciding the treatment plan.

Magnetic resonance imaging (MRI) is preferred to conventional radiography since it allows visualization of soft tissues such as inflamed synovium, tendons, and tendon sheath as well as bony structures (2). Synovitis is characterized as intraarticular tissue which increases in signal intensity on T1-weighted imaging when intravenous contrast agent is injected (3). To assess synovitis accurately, use of intravenous contrast agent has therefore been recommended (4).

In a previous study, pixel-by-pixel time intensity curve (TIC) shape analysis using dynamic contrast enhanced MRI (DCE-MRI) was proposed to be a useful method to quantify synovitis in knee and hand joints with RA without manual setting of a region of interest (ROI), where the TIC shape of synovitis is characterized by early enhancement followed by washout (5,6).

In the process of synovial quantification using DCE-MRI, there is a need to carefully eliminate the artery pixels because these can lead to incorrect volumetric assessment of synovitis. For accurate localization of arterial pixels in DCE-MRI, we hypothesized that the arterial separation method equipped with mutual information (MI) was effective, as MI provides data on the difference between pre- and post-contrast images to select ideal arterial mask phase objectively. MI is often used as an index of motion correlation in dynamic studies (7) or registration in multimodal images (8). To the best of our knowledge, the application of MI for identifying the arterial phase in DCE-MRI has never been reported. This study is an initial attempt to apply MI for this purpose. To evaluate our method, we compared it with conventional methods.

The purpose of this study was to assess the feasibility of our original arterial mask subtraction method (AMSM) with MI for quantification of synovitis in RA.

Materials and Methods

Patients

Ten RA patients (9 women and 1 man; mean age, 56.8 years; range, 38-67 years) with disease duration of under 1 year were recruited. All subjects were diagnosed with RA

according to the American College of Rheumatology/European League Against Rheumatism revised 2010 criteria (9). These patients underwent DCE-MRI of the hand for pretreatment evaluation of disease activity. This study obtained ethic board permission and informed consent from all patients.

MRI protocols

Eight patients were scanned with a 3.0 tesla MR imager (Discovery MR750w; GE Medical Systems, Milwaukee) with three-dimensional contrast-enhanced liver acquisition with volume acceleration (LAVA) dynamic sequence (repetition time/echo time 7.769–9.114/2.328–2.604 ms, slice thickness 2.0 mm, matrix size 512×512, field of view 160×160 mm, bandwidth 244.141 Hz per pixel, flip angle 12°, acquisition time per phase 13.27 s, number of slices 40 or 52, phase 26, coronal orientation). Contrast agent (0.2 ml per kg of body weight of gadopentetate dimeglumine (Magnevist®; Bayer Healthcare, Osaka, Japan) was injected by an automatic MR injection device (SonicShot GX; Nemoto Kyorindo Co. Ltd, Tokyo) at the time of 1st phase acquisition. All images involved the dominate hand with stronger clinical symptoms of RA. Patients were set in a prone position while extending the dominant arms over the head.

Two patients were scanned with a different 3.0 tesla MR imager

(Achieva; Philips Medical Systems, Eindhoven) with mDixon dynamic sequence (repetition time/echo time 13.94/0.859 ms, slice thickness 3.0 or 2.5 mm, matrix size 512×512, field of view 250×250 mm, bandwidth 1085 Hz per pixel, flip angle 10°, acquisition time per phase 8.029 or 7.490 s, number of slices 18, phase 40, coronal orientation). Contrast agent (0.2 ml per kg of body weight of gadopentetate dimeglumine (Magnescope®; Guerbet, Paris) was injected by an automatic MR injection device (SonicShot GX; Nemoto Kyorindo Co. Ltd, Tokyo) at the time of 1st phase acquisition. These images involved the bilateral hands. Patients were set in a prone position while extending both arms over their head.

Manual outlining

Manual outlining was adopted in this study as a reference standard of synovitis measurement (10). This method is widely considered reliable for assessment of synovitis with RA utilizing direct measurement by an expert of diagnosis in RA (6). Manual outlining was performed for all 344 slices by a musculoskeletal radiologist (TK) with more than 20 years of experience using a computer mouse on an image viewer (EV Insite S; PSP Corporation, Tokyo, Japan). For assessment of synovitis, DCE-MR images acquired over 5 minutes after starting contrast injection were selected.

Optimization of classifiers for TIC shape

TICs were created utilizing a median filter for smoothing purposes. TIC shape type was determined by 5 classifiers as follows (11) (Fig.1): 1, ME, “maximum enhancement” which focuses on the strongest relative signal intensity; 2, TTP, “time to peak” which focuses on the moment of ME; 3, MSI, “maximum slope increase” which focuses on the strongest enhancement between adjacent phases; 4, ISE, “initial signal excess” which focuses on the curvature of the TIC after the moment of maximum enhancement; 5, RelFS, “relative final slope” which focuses on the behavior of TIC change in the later phases. To optimize these classifiers for carpal and finger joints, 1-5 points of one pixel per patient were selected from typical regions of synovitis and artery in all subjects with a total of 35 and 40 points, respectively. The mean value of each classifier in 3 × 3 pixels of square shape with the selected pixel at the center was calculated.

The ME classifier was discarded because of, according to our experience, its limited ability to differentiate among artery, synovitis and the other tissues. Following a previous study (11), to distinguish among artery, synovitis and the other tissues, one or two thresholds were set for each classifier. For TTP and MSI, two thresholds were set because the values for these classifiers tend to fall between those of

artery and the other tissues. In contrast, for ISE and RelFS, only one threshold was assigned: ISE, reflecting washout phase at an earlier phase, can effectively differentiate artery versus synovitis; RelFS, reflecting washout phase at a later phase, can effectively differentiate artery/synovitis versus other tissues. The threshold of each classifier was derived from the mean ± 1 SD of the artery or synovitis sample group.

AMSM

AMSM was originally developed in this study to eliminate artery pixels. We hypothesize that our parameter settings for DCE-MRI allows us to capture such a phase in which only the artery is enhanced by intravenous contrast agent during acquisition of DCE-MRI. By utilizing the image at the phase of "exclusive arterial enhancement" as an image mask, arterial pixels can be eliminated from TIC shape analysis (Fig.3). Here, the phase of exclusive arterial enhancement in DCE-MRI must be decided very carefully. To facilitate this in an objective manner, MI was introduced. MI has been applied representing the similarity between two images. The formula for the calculation of MI is (12)

$$MI = \sum_{i_1} \sum_{i_2} p(i_1, i_2) \log_2 \frac{p(i_1, i_2)}{p(i_1) p(i_2)},$$

where p(i_1, i_2), p(i_1,), p(i_2) are joint and individual intensity probability distributions, and i_1, i_2 are the intensities of the input and target image, respectively.

We obtained 26 phases after contrast administration in this DCE-MRI study. Phase 1 was a pre-contrast image as it was obtained simultaneously with contrast administration. We defined the MI between phase 1 (pre-contrast) and phase n as MI (n). In addition, ΔMI(n) was defined as MI(n)-MI(n-1). To simplify and accelerate the MI calculation, image data was replaced with a 256-step gray scale.

For comparison purposes, we also examined two facile approaches to objective mask phase selection: 1, selection using uniform phase, which was determined with the same mask phase in all data (2~6th phase after pre-contrast); 2, selection using the phase to peak (PTP) in arterial TIC, which determined the phase representing the highest signal intensity in the ROI (approximately 10 pixels) placed on the radial artery.

Statistical analysis

Synovitis area per each slice (n = 344) and volume per patient (n = 10) were measured by our original software developed with Microsoft Visual C# 2013 using the Microsoft Foundation Classes. Pixels having TIC shape type 4, which is characterized as early

enhancement followed by washout phase, were regarded as synovitis pixel (13,14). The validity of the combination of TIC shape analysis and AMSM was compared with manual outlining defined as a reference of standard using Pearson's correlation coefficient. Criteria for Pearson's correlation coefficient were defined as follows: $r<0.2$, poor; $0.2 \leqq r<0.4$, fair; $0.4 \leqq r<0.6$, moderate; $0.6 \leqq r<0.8$, good; and $r \geq 0.8$, excellent and $p<0.05$, significant. Paired t-tests were performed between measurements by a combination of TIC shape analysis with AMSM and that by TIC shape analysis without AMSM to examine the accuracy of assessment in slices without synovitis pixels ($p<0.05$, significant). The intra-class correlation coefficient (ICC) between subjective and different objective selections of mask phase was calculated to test the agreement between them. Criteria for ICC were defined as follows: $ICC<0.2$, poor; $0.2 \leqq ICC<0.4$, fair; $0.4 \leqq ICC<0.6$, moderate; $0.6 \leqq ICC<0.8$, substantial; and $ICC \geq 0.8$, almost perfect.

Results

Optimization of classifiers for TIC shape

Fig.3 shows the results for the distribution of classifiers. There were changes of threshold from a previous study in all classifiers (Table 1). The threshold of ME was furthermore set to 1.0. This threshold is higher than that of the previous study (11) since

acquisition time for single phase of the current study (approximately 13 seconds) was shorter than that of the previous study (21 seconds) (11). It is likely that more noise was included in images of the current study due to its shorter acquisition time. To exclude the contribution of noise from analysis as much as possible, a higher threshold was used. TIC shape analysis using optimized threshold of classifier for hand was then found to correlate better ($r=.723$, $p<0.01$) than previous TIC shape analysis for knee ($r=.213$, $p=0.03$).

Combination of TIC shape analysis and AMSM

Decreasing the MI (n) value and the spreading of the distribution of 2D histograms were recognized after injection of contrast agent (Fig. 4). Similarity between pre-contrast and post-contrast images declined as shown in Fig. 5; MI (n) changed along with intake of intravenous contrast agent. The phase of DCE-MRI entering the plateau was defined as the arterial mask phase. To decide this phase, three thresholds for ΔMI (n) were set (10%, 5%, and 1% to maximum ΔMI (n)). The mask phase selected objectively based on reference threshold was compared with subjective assessment, which was a selection of the arterial mask phase by a radiological technologist with 2 years' experience. The efficacy of smoothing the Phase/MI graph using a simple moving average filter was also

investigated. Time needed for AMSM and TIC was 30.8 ± 2.24 and 74.4 ± 3.37 seconds, respectively.

Agreement between subjective and objective selection of the arterial mask phase is shown in Table 2. The variation of 5% for maximum ΔMI value as well as the application of a simple moving average filter were more suitable for searching for the plateau (ICC = 0.734, $p < 0.05$) than other threshold settings. Comparing among objective selections (Table 3), selection utilizing MI had superior correlation for volumetry of synovitis ($r = 0.921$, $p<0.01$).

In terms of slice by slice assessment for slices without synovitis pixels (n = 113) determined by manual outlining, the average number of synovitis pixels was significantly lower for TIC shape analysis with AMSM than TIC shape analysis without AMSM (Fig.6).

Discussion

TIC shape analysis for dynamic MRI in RA patients was first introduced by Leij, who identified relevant TIC shape to RA in the MRI of the knee (14). This previous study proved that pixels related with RA or TIC shape of “wash-in and wash-out” had strong correlation with synovitis pixels in the hand (5). In the current study, we optimized the

parameters of TIC shape analysis for quantification of synovitis in the hand region of RA. Furthermore, we improved the TIC shape analysis using AMSM, which can avoid errors of selecting arterial pixels in the process of depicting synovitis pixels. This may indicate that miss-classification of arteries as synovitis was decreased because the artifacts from partial volume effect in the pixels of perivascular tissue were reduced by AMSM.

As for the results of optimization of classifiers, all classifiers thresholds needed to be changed from those in the previous study (11). This might be derived from the differences in the TIC for artery of DCE-MRI between the previous axial knee study and our coronal hand study. Contrary to axial images, coronal images include arteries of different proximity in the same slice, which may cause diverse TTP in the artery. In fact, TTP of this study was delayed from the previous study (80 s and 40 s, respectively) (11).

As for objective selection of appropriate arterial phase for mask subtraction, MI led to better agreement with subjective selection than the other methods. Although the pixels of different phase of enhancement were included in the same slice, MI, a measure of the mutual dependence between the two variables, could assess difference in enhancement between images of 2 different phases for the entire images. In contrast,

selection using ROI setting on the radial artery had inferior agreement with subjective selection since it might be affected by limited ROI size.

This study was limited by the small number of patients. Although the group of patients included different kinds of disease activity, recruiting more various patients will lead to better assessment of feasibility. In addition, motion correction for DCE-MRI was not applied. Patients were carefully instructed to stabilize themselves as much as possible. Nevertheless, body motion during acquisition time (5~6 minutes) may adversely affect TIC shape analysis.

In conclusion, the combination of TIC shape analysis and image subtraction can accurately quantify synovitis of RA by eliminating arterial pixels in the hand region. MI may be feasibly applied as an objective index for arterial phase determination in DCE-MRI.

References

1. van der Heijde DM. Radiographic imaging: the 'gold standard' for assessment of disease progression in rheumatoid arthritis. Rheumatology (Oxford) 2000;39 Suppl 1:9-16.

2. Dohn UM, Ejbjerg BJ, Hasselquist M, et al. Detection of bone erosions in rheumatoid arthritis wrist joints with magnetic resonance imaging, computed tomography and radiography. Arthritis Res Ther 2008;10(1):R25.

3. Lavini C, Buiter, Maas. Use of dynamic contrast enhanced time intensity curve shape analysis in MRI: theory and practice. Reports in Medical Imaging 2013.

4. Kursunoglu-Brahme S, Riccio T, Weisman MH, et al. Rheumatoid knee: role of gadopentetate-enhanced MR imaging. Radiology 1990;176(3):831-835.

5. Sakashita T, Kamishima T, Kobayashi Y, et al. Accurate quantitative assessment of synovitis in rheumatoid arthritis using pixel-by-pixel, time-intensity curve shape analysis. Br J Radiol 2016;89(1061):20151000.

6. Savnik A, Bliddal H, Nyengaard JR, Thomsen HS. MRI of the arthritic finger joints: synovial membrane volume determination, a manual vs a stereologic method. Eur Radiol 2002;12(1):94-98.

7. Hodneland E, Lundervold A, Rorvik J, Munthe-Kaas AZ. Normalized gradient fields for nonlinear motion correction of DCE-MRI time series. Comput Med Imaging Graph 2014;38(3):202-210.

8. Maes F, Collignon A, Vandermeulen D, Marchal G, Suetens P. Multimodality image registration by maximization of mutual information. IEEE transactions on medical imaging 1997;16(2):187-198.

9. Aletaha D, Neogi T, Silman AJ, et al. 2010 Rheumatoid arthritis classification criteria: an American College of Rheumatology/European League Against Rheumatism collaborative initiative. Arthritis Rheum 2010;62(9):2569-2581.

10. Ostergaard M. Different approaches to synovial membrane volume determination by magnetic resonance imaging: manual versus automated segmentation. British journal of rheumatology 1997;36(11):1166-1177.

11. Lavini C, de Jonge MC, van de Sande MG, Tak PP, Nederveen AJ, Maas M. Pixel-by-pixel analysis of DCE MRI curve patterns and an illustration of its application to the imaging of the musculoskeletal system. Magn Reson Imaging 2007;25(5):604-612.

12. Crabb MG, Davidson JL, Little R, et al. Mutual information as a measure of image quality for 3D dynamic lung imaging with EIT. Physiol Meas

2014;35(5):863-879.

13. Kim EY, Kwack KS, Cho JH, Lee DH, Yoon SH. Usefulness of dynamic contrast-enhanced MRI in differentiating between septic arthritis and transient synovitis in the hip joint. AJR American journal of roentgenology 2012;198(2):428-433.

14. van der Leij C, van de Sande MG, Lavini C, Tak PP, Maas M. Rheumatoid synovial inflammation: pixel-by-pixel dynamic contrast-enhanced MR imaging time-intensity curve shape analysis--a feasibility study. Radiology 2009;253(1):234-240.

Table

Table1 Modified thresholds for time intensity curve shape analysis after optimization to hand region from knee MRI study (14)

Type	TTP(s)	MSI	ISE	RelFS
2	> 180	< MSD / 2.8		> - 0.001
	> 180	< MSD / 2.0		> 0.15
3		> MSD / 2.8		-0.0001 < FS < 0.0001
		> MSD / 2.0		-0.015 < FS < 0.015
4	< 180	> MSD / 2.8	< 0.8	< -0.0001
	< 180	> MSD / 3.0	< 1.3	< -0.015
5	> 180	> MSD / 2.8		> 0.0001
	> 180	> MSD / 2.0		> 0.015
6	< 80	> MSD / 1.75	> 0.8	< -0.0001
	< 40	> MSD / 2.0	> 1.3	< -0.015

For each TIC shape type, thresholds for the hand from current study and knee joint from a previous study are shown in the top and the bottom, respectively. TIC shape type 4, definition of TIC shape type of synovitis. TTP, time to peak; MSD, maximum signal

difference; MSI, maximum signal increase; ISE, initial signal excess; RelFS, relative final slope.

Table 2 Agreement between subjective and objective selection of arterial mask phase

		Without smoothing			With smoothing			
PT No.	Manual	10%	5%	1%	10%	5%	1%	PTP
1	4	3†	3†	6	3†	4*	7	7
2	3	2†	2†	5	3*	3*	5	4†
3	3	2†	4†	7	3*	3*	12	4†
4	3	2	3*	8	3*	3*	3*	4†
5	5	2	2	4†	3	4†	9	4†
6	4	3†	3†	6	3†	3†	7	7
7	5	3	3	3	3	4†	7	7
8	4	4*	4*	4*	4*	5†	11	5†
9	4	2	2	2	3†	3†	9	6
10	6	2	2	2	3	6*	7†	7†
ICCs	NA	0.000	-0.250	-0.658	-0.230	0.734‡	-0.187	0.301

PT No., patient number; *, perfect agreement; †, adjacent to manual; ‡, $p<0.05$; PTP, phase to peak. ICCs, intra-class correlation coefficients; NA, not applicable

Table 3 Comparison of correlation among different manners of mask selection

	Simple TIC	Combination methods						
Arterial mask selection	No mask	Uniform selection 2	3	4	5	6	PTP	MI
r	.891	.871	.877	.827	.799	.745	.899	.921
p	>0.01	>0.01	>0.01	>0.01	>0.01	0.013	>0.01	>0.01

TIC, time intensity curve; PTP, phase to peak; MI, mutual information.

Figure Legends

Figure 1 Definition and concept of TIC classifiers.

Figure was adapted from a previous study (11). TIC types were defined by 5 classifiers. The formula to calculate classifiers is shown at the top right. α, intercept of the line fitted to the last scan, β, tangent of the line fitted to the last scan; SB, signal base; MSD, maximum signal difference; ME, maximum enhancement; TTP, time to peak; MSI, maximum signal increase; ISE, initial signal excess; RelFS, relative final slope.

Figure 2 Concept of Arterial Mask Subtraction Method

Upper row shows flow of DCE-MRI. The artery is initially enhanced (red pixels). Inflamed synovium (green pixels) as well as other tissues (not shown here) are then enhanced. Lower row shows the concept of arterial mask subtraction method.

Arterial pixels are subtracted from equilibrium phase image. The other tissues including inflamed synovium (green pixels) remain.

Figure 3 Distribution of TIC shape type classifiers and thresholds

Dot-dash line shows the thresholds between artery and synovitis. Dotted line shows the

thresholds between synovitis and other tissues. Straight line shows the thresholds of washout. Left box shows distribution of classifiers for artery. Right box shows distribution of classifiers for synovitis. These thresholds were derived from a sample group of artery and synovitis.

Figure 4 Spreading 2D histogram along with acquisition of DCE-MRI

a, Image of DCE-MRI in the 1st phase. This was regarded as a pre-contrast image. b, Image of DCE-MRI in the 2nd phase. c, Image of DCE-MRI at 3 minutes. Synovitis was clearly enhanced. d, 2D histogram of coordinate combination between image(a) and image(b). The two images corresponded perfectly. 2D histogram expressed as a line. e, 2D histogram of coordinate combination between image(a) and image(b). 2D histogram was spread slightly. f, 2D histogram of coordinate combination between image (a) and image (c). 2D histogram was spread more. 2D histogram was spread along with the progression of DCE-MRI. The MI value also decreased.

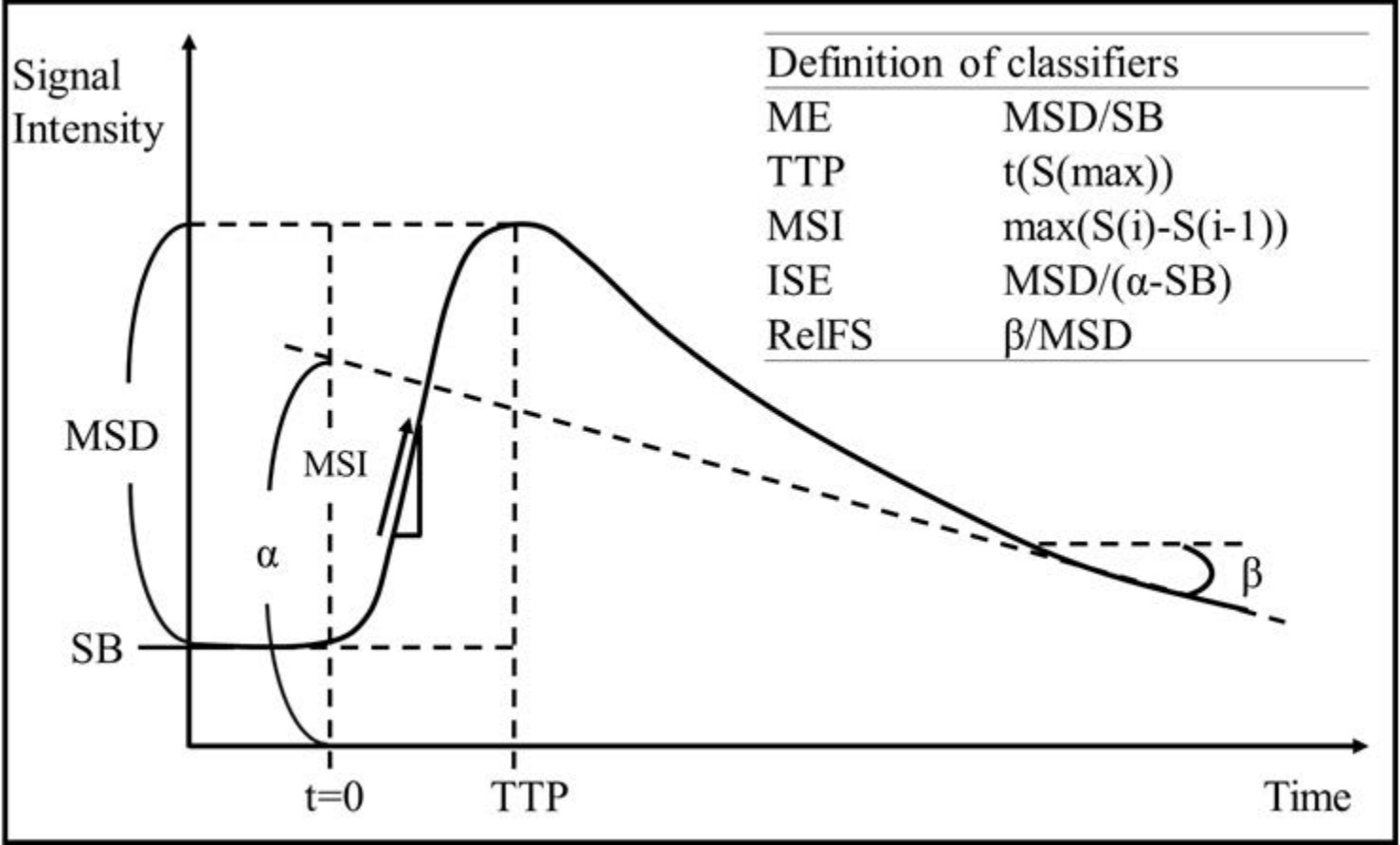
Figure 5 Change of mutual information value in DCE-MRI

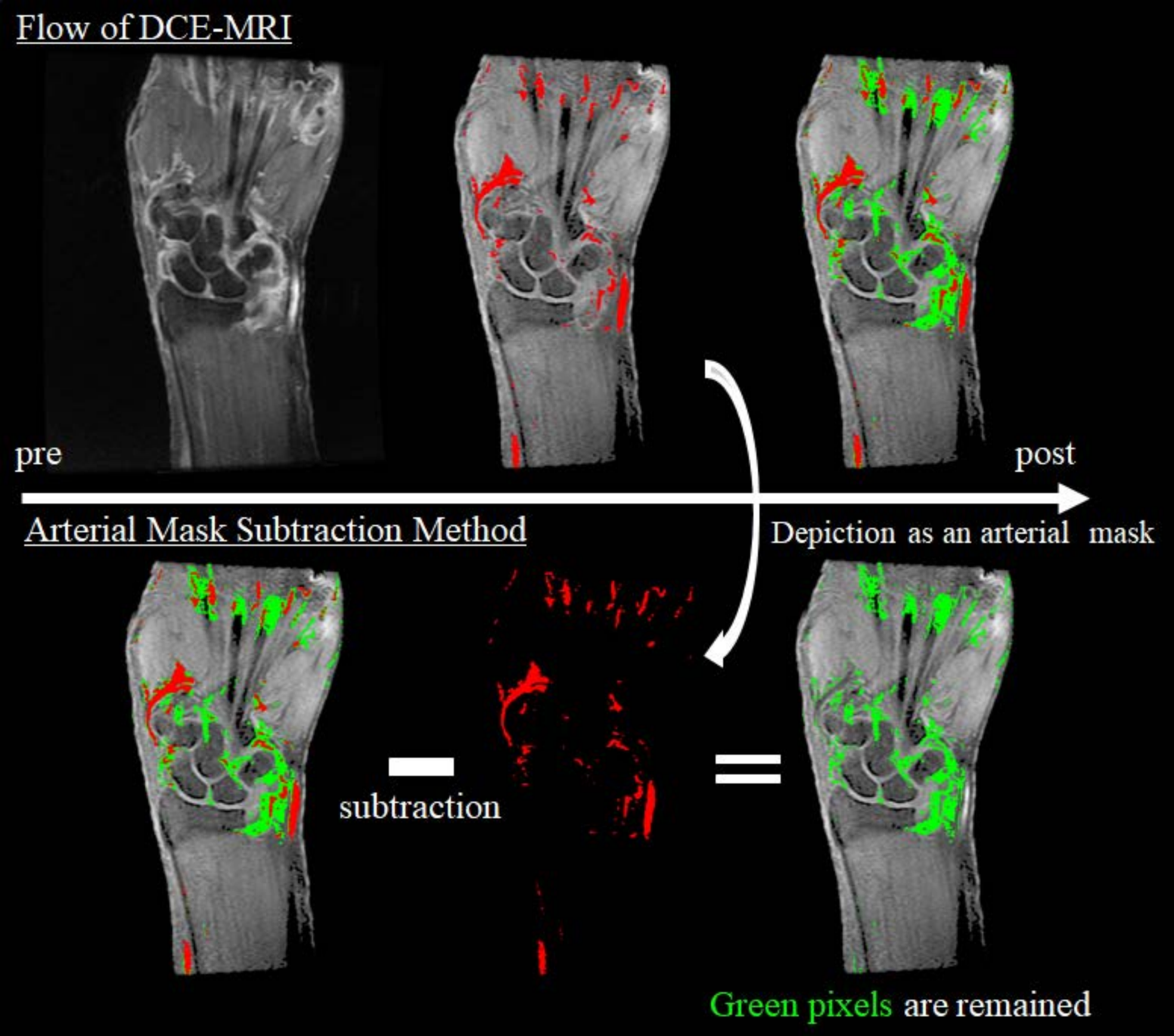
Left graph shows the change of the mutual information (MI) value after contrast

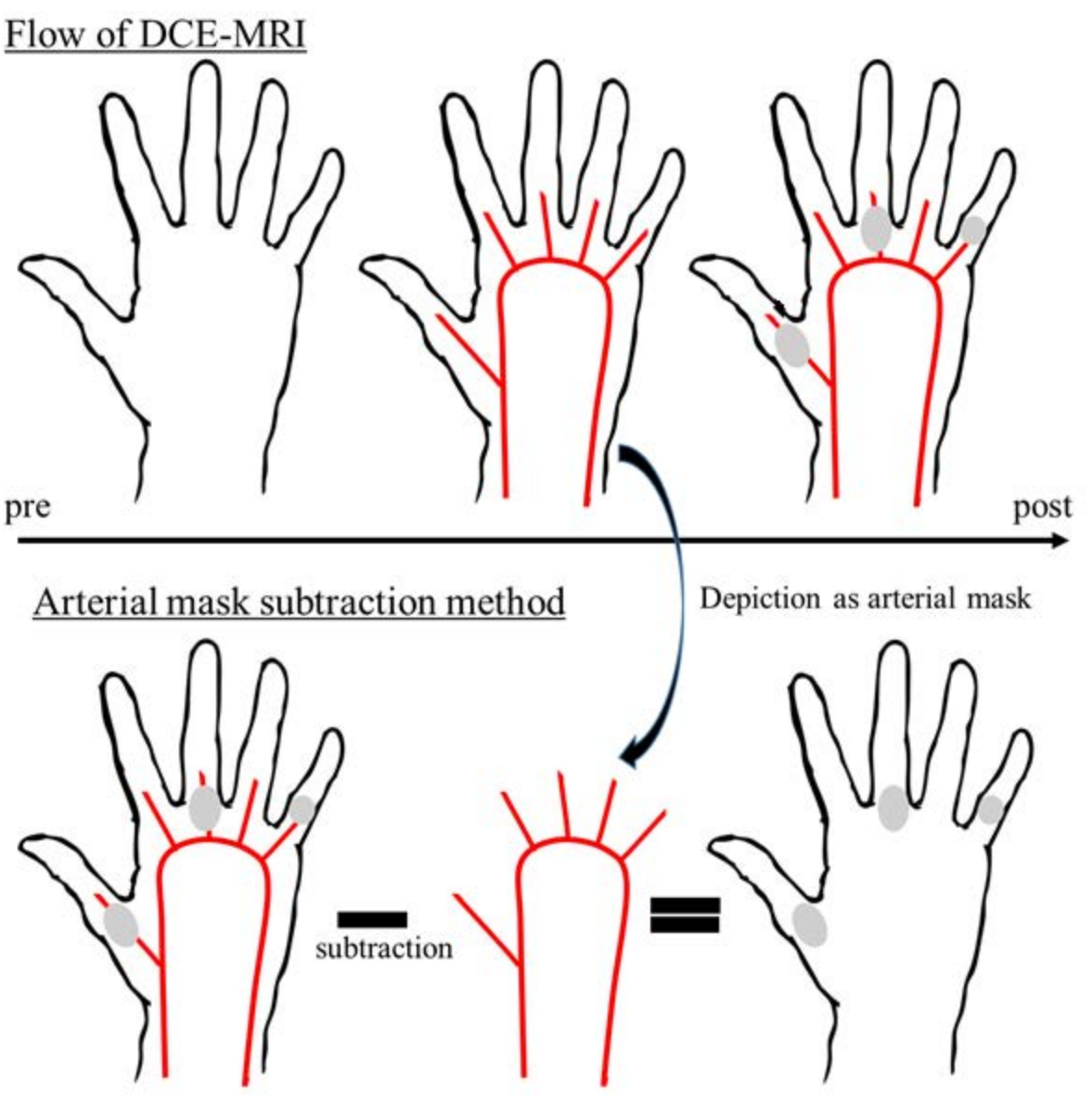
administration. MI for the 1st phase vs. the 1st phase was the highest. Decreasing MI value was also observed. Right graph shows the detail change of MI value in the 2nd to the 14th phase. Subjective selection of mask phase by observing DCE-MRI was at the 3rd phase. At the 4th phase, the plateau already appears to have begun.

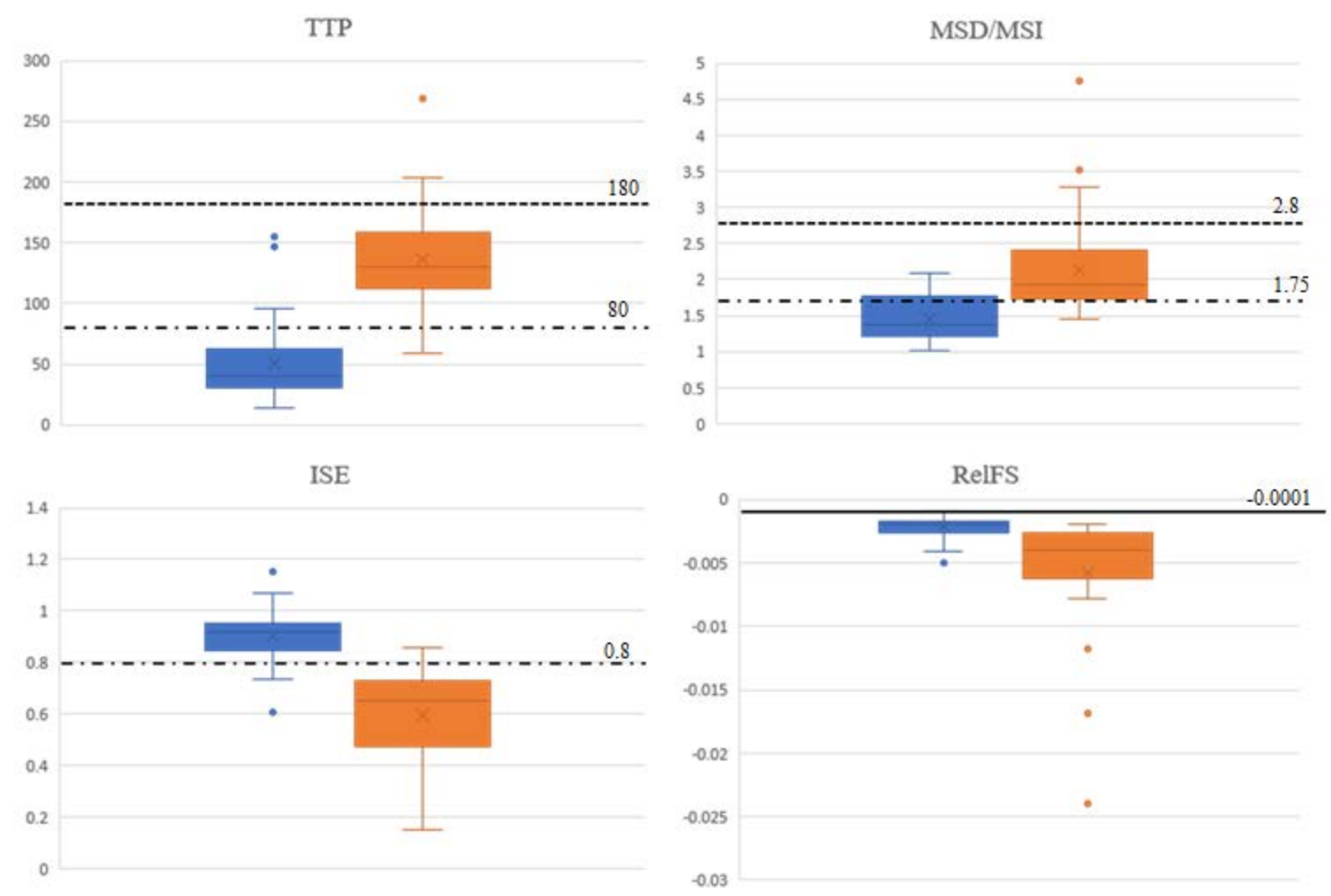
Figure 6 Comparison of measurement of synovitis in slices without synovitis between two TIC shape analyses

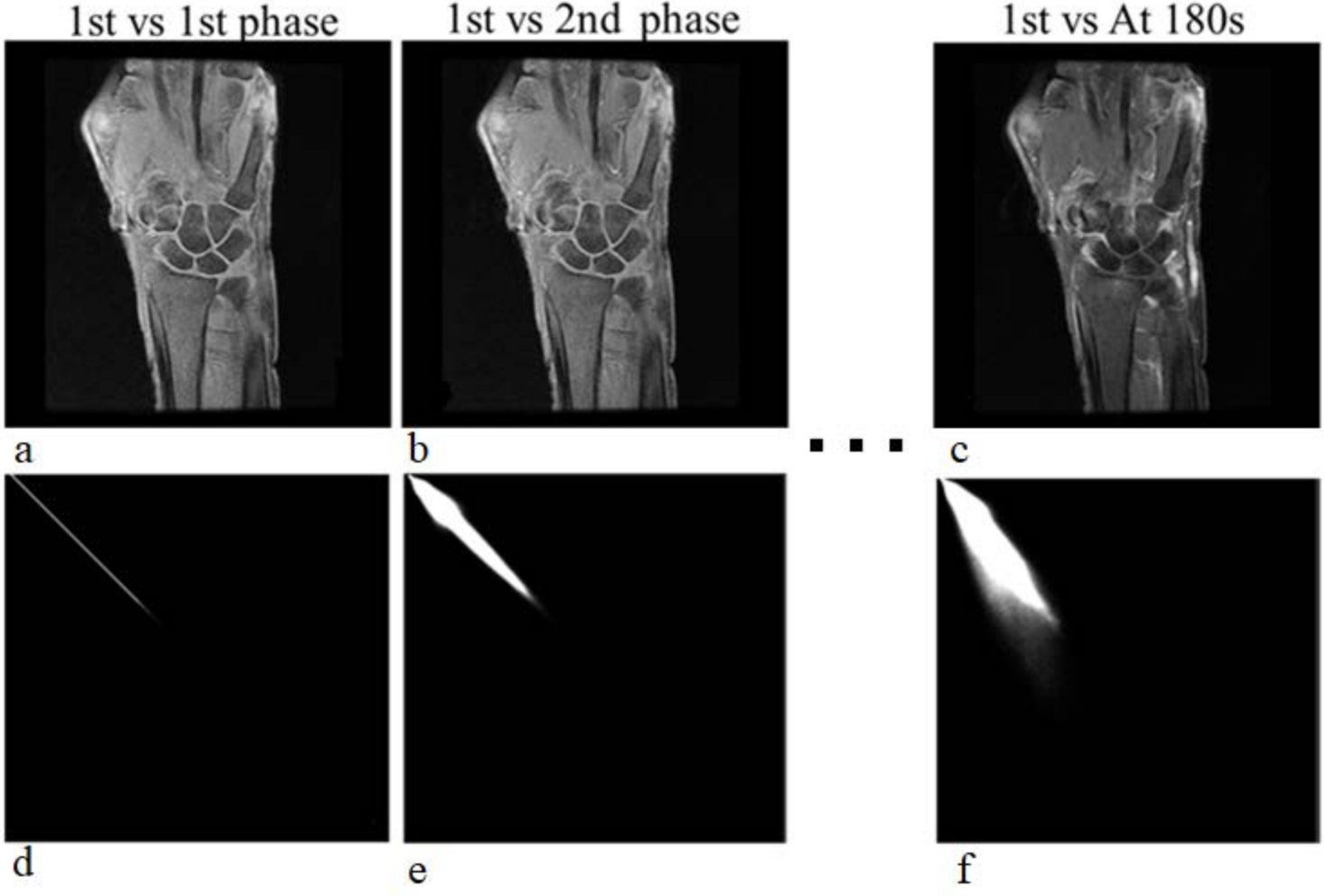
Combination of TIC shape analysis and arterial mask subtraction method could accurately assess slices without synovitis. Significantly lower volume of synovitis was detected via TIC analysis with the arterial mask subtraction method than that without.

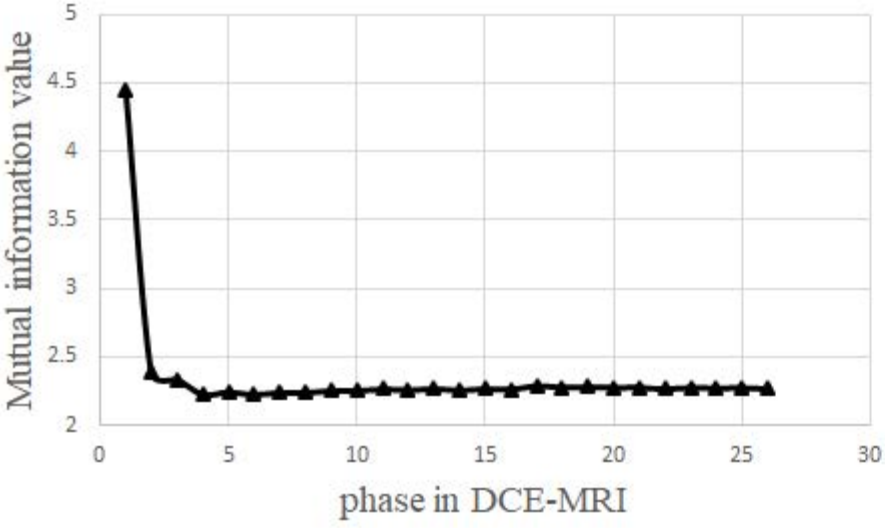

Signal Intensity
MSD
SB
MSI
α
β
t=0
TTP
Time
Definition of classifiers
ME MSD/SB
TTP t(S(max))
MSI max(S(i)-S(i-1))
ISE MSD/(α-SB)
RelFS β/MSD

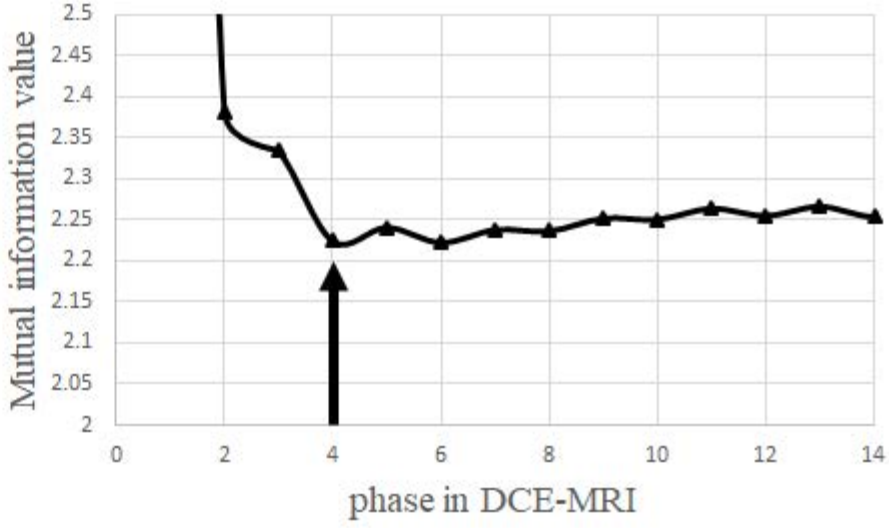

Flow of DCE-MRI
pre
post
Arterial Mask Subtraction Method
Depiction as an arterial mask
subtraction
Green pixels are remained

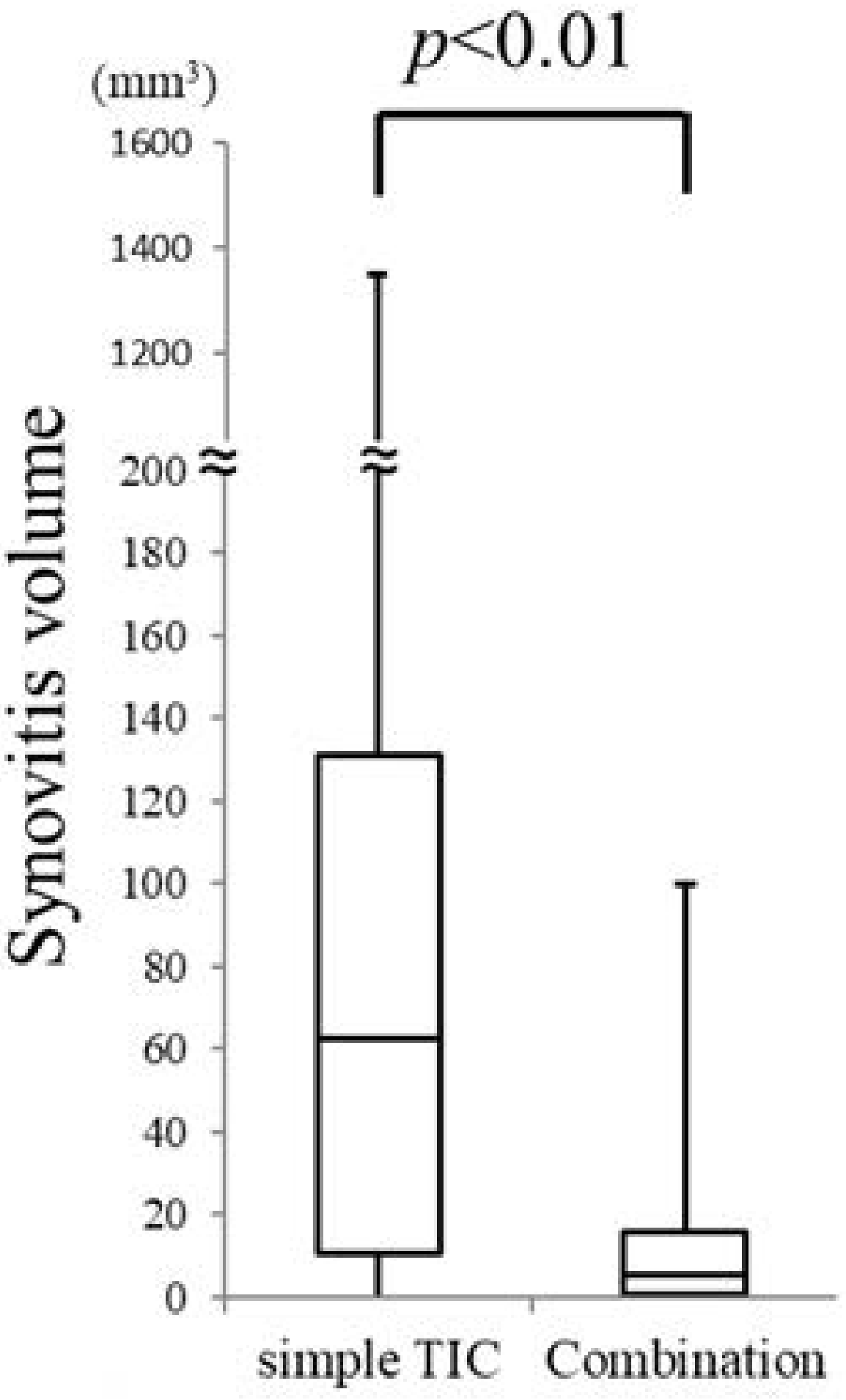

Flow of DCE-MRI
pre
post
Arterial mask subtraction method
Depiction as arterial mask
subtraction


TTP
300
250
200
150
100
50
0
180
80
MSD/MSI
5
4.5
4
3.5
3
2.5
2
1.5
1
0.5
0
2.8
1.75
ISE
1.4
1.2
1
0.8
0.6
0.4
0.2
0
0.8
RelFS
0
-0.005
-0.01
-0.015
-0.02
-0.025
-0.03
-0.0001


1st vs 1st phase
1st vs 2nd phase
1st vs At 180s
a
b
c
d
e
f


Mutual information value
5
4.5
4
3.5
3
2.5
2
0
5
10
15
20
25
30
phase in DCE-MRI


Mutual information value
2.5
2.45
2.4
2.35
2.3
2.25
2.2
2.15
2.1
2.05
2
0
2
4
6
8
10
12
14
phase in DCE-MRI


p<0.01
(mm3)
1600
1400
1200
200
180
160
140
120
100
80
60
40
20
0
Synovitis volume
simple TIC
Combination